

## The giant moment of $PdMn$ at very low temperature

J. Flouquet, M. Ribault, O. Taurian, and J. Sanchez

*Laboratoire de Physique des Solides, Orsay, France*

J. L. Tholence

*Centre de Recherche des Très Basses Températures, Grenoble, France*

(Received 26 April 1976; revised manuscript received 28 February 1977)

Magnetization and nuclear orientation experiments on dilute alloys of  $PdMn$  allow the first observation of the giant moment of the manganese impurity down to 10 mK without Kondo-like coupling. Below 10 mK, spin-glass magnetic interactions occur due to iron parasitic impurities even for an alloy containing no more than 3 ppm of iron. The nuclear orientation results are compared with those obtained for a  $AuMn$  alloy which has almost the same hyperfine constant.

### INTRODUCTION

Recently Star *et al.*<sup>1</sup> have shown that the magnetic properties of a manganese impurity dissolved in a Pd lattice can be described by a giant moment of  $7.5\mu_B$ . They performed static magnetization measurements down to 1.4 K for concentrations of 500 ppm and above. As in  $PdFe$  and  $PdCo$  alloys, an important fraction of the magnetization is due to moments induced on the palladium atoms.

We have performed nuclear-orientation (NO) experiments on dilute alloys of  $PdMn$  in order to obtain information on these alloys at more than two orders of magnitude lower temperature and concentration.

When the electronic magnetization is fully saturated in high magnetic fields, a nuclear-orientation measurement indicates the value of the local moment on the impurity site through the hyperfine constant  $A$ . At very low concentration, where the magnetic coupling between the impurities can be neglected, the NO response at low applied fields will be sensitive to the coupling between the local moment and the conduction electrons. As has been reported for many dilute alloys,<sup>2</sup> if a Kondo coupling occurs above the experimental range of temperature, the NO response is strongly reduced from its free paramagnetic behavior (strong Kondo coupling). On the other hand, the occurrence of a giant moment well above the Kondo temperature, must lead to an enhancement of the bare electronic Zeeman term which would be attributed to the local moment without taking into account the long-range polarization of the lattice. The present measurement is the first attempt to observe by NO at very low temperatures the ground state of an impurity which carries a giant moment at higher temperatures.

Finally, the study of a more concentrated alloy will show the sensitivity of the NO to the orienta-

tion of the local symmetry axis of the magnetic coupling with respect to the macroscopic symmetry axis defined by the applied field  $H$ .<sup>3</sup>

### EXPERIMENTAL CONDITIONS

We have taken care to minimize the presence of magnetic impurities other than manganese. Thus, the commercial  $^{54}MnCl_2$  activity was cleaned by separation with ether in order to eliminate any iron atoms present in the radioactive solution. The cleaned activity was electroplated or directly painted on a Pd wire which has a nominal purity better than 99.999% (manufactured by Johnson Matthey). The Pd samples were then melted under vacuum using a high-frequency furnace on a water-cooled copper hearth. No differences have been observed for the two types of depositions. For the preparation of the  $AuMn$  alloys which were studied as a NO reference signal, we have observed an attenuation of the NO signal in low fields when the sample was melted without preliminary decomposition of the  $MnCl_2$  activity in comparison with the signal obtained after a separation of the Mn and Cl atoms. The reference signal was taken from the latter procedure.

The high energy of the observed  $\gamma$  rays (835 keV) means that the samples can be made of bulk materials usable for other techniques. The weight of the melted sample was typically 0.5 g. In order to avoid any doubt about the purity of the samples, firstly we have performed magnetization measurements which determine the content  $C_m$  of all magnetic impurities dissolved in the lattice together with their polarization as a function of the applied magnetic field  $H$ ; secondly, using neutron activation analysis, we have verified that  $C_m$  is due to iron impurities. The concentration of the radioactive Mn impurities is much lower than 1 ppm, and is always lower than the parasitic iron concen-

tration C.

The magnetization experiments, performed in Grenoble, were done in the range of temperature 50 mK–4K with applied fields up to 3 kOe.

The NO experiments were performed with an adiabatic demagnetization cryostat. With a cerium-magnesium-nitrate (CMN) salt, the temperature of the sample takes five hours to rise from 3 to 10 mK; with a chrome alum salt, the temperature rises from 10 to 20 mK in over 12 hours. The temperature was measured by a NO Co<sup>60</sup>Co single-crystal thermometer. As the hyperfine field of Co in domains of a hexagonal Co crystal is not well established, in preliminary experiments we have determined its value to be –227 kOe using a Ni<sup>54</sup>Mn NO thermometer.<sup>4</sup> The polarization of the samples was obtained either in a low-field magnet with no remanent field or in a high-field magnet which gives fields up to 40 kOe. The  $\gamma$  rays are detected by a planar Ge(Li) detector mounted along  $H$ . The corrections for the background and for the electronic drift are performed by a computer.<sup>4</sup> The solid angle corrections have been determined by extrapolation of the value calculated by Avignone *et al.*<sup>5</sup> The warm counts are measured between each cooling salt-magnetization procedure during more than one hour with the same experimental conditions as those of the cold counts.

In order to avoid any disturbance of the magnetic field on the Ge(Li) detector, each run, including the warm count, is made at constant field  $H$ . We have verified that we find for the AuMn alloy the same saturation hyperfine field as previously obtained by Williams<sup>6</sup> and Lagendijk *et al.*<sup>7</sup> who used NaI(Tl) counters along  $H$  and perpendicular to  $H$ . The experimental anisotropy is measured with an uncertainty  $\Delta E$  better than 0.5%; the corresponding accuracy on the hyperfine field is better than 3%.

#### REPRESENTATION OF THE RESULTS

If the Hamiltonian of the parent nuclei has a cylindrical axis of quantization  $Z$ , the angular distribution of the  $\gamma$  rays emitted at angle  $\theta$  with respect to the  $Z$  axis is given by the general expression (see Ref. 8)

$$W(\theta) = \frac{N_c(\theta)}{N_w(\theta)} = \sum_K g_K U_K F_K B_K P_K(\cos\theta), \quad (1)$$

where  $N_c(\theta)$ ,  $N_w(\theta)$  represent respectively the cold and warm counts;  $g_K$  is a solid angle correction which characterizes the detector;  $U_K F_K$  are nuclear parameters which describe the unobserved transitions;  $P_K(\cos\theta)$  is a Legendre polynomial and  $B_K$  the nuclear orientation parameter which is related to the population of the parent nuclear sub-levels.

For the <sup>54</sup>Mn nuclei, the coefficients  $U_K F_K$  are well known; Fig. 1 represents the  $\gamma$  distribution of the 835-keV  $\gamma$  ray emitted by <sup>54</sup>Mn nuclei which are subjected to a magnetic field of 200 kOe along the  $Z$  axis. We note the high sensitivity at low temperature to any angle  $\theta$  of misalignment between the axis of the detector and the local  $\hat{Z}$  axis of quantization. If the local axis of quantization of each nucleus coincides with the macroscopic axis  $Z_0$  defined by the applied field  $H$ , all solid-state information is contained in the orientation parameter  $B_K$ . The experimental results will be compared with the theoretical values computed for different NO mechanisms. When the macroscopic axis does not coincide with the local axis, misalignment effects must be taken into account and the expression (1) must be computed for each local axis.<sup>2</sup>

The experimental results are initially expressed as the measured axial  $\gamma$  anisotropy along  $H$  which is defined by

$$E(0) = [N_w(0) - N_c(0)] / N_w(0).$$

The second part of the analysis expresses the axial anisotropy in terms of an effective field,  $H_{\text{eff}}$  oriented along the applied field.  $H_{\text{eff}}$  is that magnetic field, acting on the nuclei along the magnetic field axis  $\hat{Z}_0$ , which would give the same anisotropy as the observed anisotropy  $E(0)$ . It corresponds to the value  $E(0)$  calculated from a brute-force Hamiltonian:

$$\mathcal{H} = g_n \mu_n H_{\text{eff}} I_{Z_0}.$$

The advantage of this representation is that when the symmetry of the external field breaks down

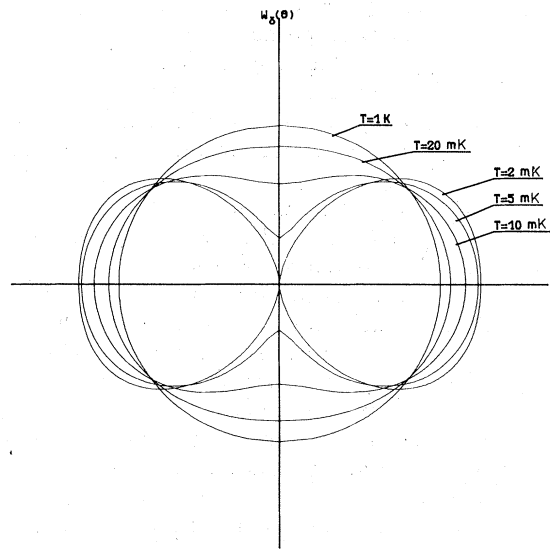


FIG. 1. Distribution of the 835-keV  $\gamma$  ray of a <sup>54</sup>Mn probe submitted to a hyperfine field of 200 kOe.

locally, striking results appear on the temperature dependence of the effective field. NO is thus an excellent test of an eventual local breakdown of the macroscopic symmetry. In a paramagnetic regime, where  $\hat{Z}$  coincides with  $\hat{Z}_0$ ,  $H_{\text{eff}}$  is almost independent of  $1/T$  whatever the strength of the magnetic field and the strength of the ratio  $k_B T_K/A$ .<sup>2</sup> If interactions among impurities occur as in a spin glass, the local  $\hat{Z}$  axis does not coincide with  $\hat{Z}_0$ , but is oriented along the vector sum  $\vec{H}_r$  of the applied field  $\vec{H}$  and the molecular field  $H_m$  which is randomly distributed. Table I shows the values of  $H_{\text{eff}}$  as a function of  $T^{-1}$  calculated with the assumptions of a hyperfine field of  $-400$  kOe and of a randomly oriented molecular field  $H_m = 0.5H$ ; we assume that the electronic magnetization is saturated for each site in the local field  $\vec{H}_r$ . The main result, that can be observed, is the decrease of  $H_{\text{eff}}$  with increasing  $1/T$ . We emphasize here that the NO experiments are more sensitive to the misalignment ( $\hat{Z}, \hat{Z}_0$ ) than are the magnetization experiments which follow a  $\cos\theta$  attenuation independent of  $1/T$ . In order to give an order of magnitude, if we take as an example the case described by Fig. 1, a misalignment of  $10^\circ$  leads to a reduction in the average magnetization of 1.6% only, but to an  $H_{\text{eff}}$  which drops by 20% when the temperature is lowered from 20 to 5 mK.

#### SATURATION HYPERFINE FIELD

When the electronic magnetization  $g\mu_B S$  is completely saturated, the impurity nuclei of spin  $I$  are submitted to an effective field equal to

$$H_{\text{eff}}(\text{sat}) = H + H_{\text{hf}}(\text{sat}),$$

where  $H_{\text{hf}}(\text{sat})$  is related to the hyperfine constant  $A$  of the free-spin Hamiltonian:

$$\mathcal{H}_0 = A \vec{I} \cdot \vec{S} + g\mu_B \vec{H} \cdot \vec{S} + g_n \mu_n \vec{H} \cdot \vec{I} \quad (2)$$

by the relation

$$H_{\text{hf}}(\text{sat}) = AS/g_n \mu_n. \quad (3)$$

The value of  $-370 \pm 10$  kOe which has been measured here agrees with that determined by Gallop<sup>9</sup> and is close to the value of  $-400$  kOe measured for Mn nuclei dissolved in gold. As the hyperfine constant reflects principally the local magnetization of the impurity, we can conclude that, at the site of the impurity, the local moment  $m_1$  of manganese

TABLE I. Variation of the effective field of a  $^{54}\text{Mn}$  nucleus submitted to a hyperfine field of  $-400$  kOe, as a function of  $1/T$  in the case of a spin-glass coupling described by a molecular field  $H_m = 0.5H$ .

$1/T$ ( $\text{K}^{-1}$ )	60	100	150	200	250	300
$H_{\text{eff}}$ (kOe)	304	260	209	172	144	120

in the palladium lattice is close to the value of  $5\mu_B$  attributed to Mn impurities in the AuMn alloys, which is described as an S state with  $S = \frac{5}{2}$ ,  $g = g_0 = 2$ .

#### SINGLE-IMPURITY EFFECTS

We emphasize here that a nuclear-orientation experiment is a purely static measurement, which is not affected by the fluctuation of the electronic spin so long as the electronic relaxation effects do not change the nuclear eigenstates and hence the density matrix which enters in the  $\gamma$  anisotropy calculation. In the absence of any Kondo coupling, whatever the electronic relaxation time  $\tau_s$  of the local moment is, the experimental anisotropy or associated effective field should fit a function  $E_g^S$  or  $H_g^S$ , respectively, calculated from the Hamiltonian  $\mathcal{H}_0$  with well-specified spin  $S$  and splitting factor  $g$ . As the two parameters  $g_n \mu_n$ ,  $I$  are well known in the Hamiltonian  $\mathcal{H}_0$ , the axial theoretical function  $E_g^S(0)$  depends on three parameters  $A$ ,  $S$ ,  $g$ . The relation (3) limits the fit to two parameters when the saturation hyperfine field is known.  $E_g^S$  (or  $H_g^S$ ) is the analog for NO to the Brillouin function  $B_g^S$  for magnetization experiments. Table II describes the  $H_2^{5/2}$  function for a  $^{54}\text{Mn}$  nuclei, submitted to a hyperfine coupling of  $-400$  kOe, for different applied fields and temperature. In contrast to the Brillouin function  $B_g^S$ ,  $H_g^S$  is almost independent of  $1/T$ . Its smooth variation with the applied field express the weak mixing by the applied field of the electron nuclear levels.

Knowing  $H_{\text{hf}}(\text{sat})$ , we compare now the experimental anisotropy or associated effective field with the calculated function  $E_g^S$ . Figure 2 shows the experimental anisotropy of a PdMn alloy containing 3 ppm of iron for three applied fields. These results are compared firstly with those obtained with a very dilute alloy of Au  $^{54}\text{Mn}$  measured in the same conditions, and secondly with the theoretical function  $E_2^{5/2}(0)$ . (We also attempted to use PdH<sub>0.7</sub>Mn as a reference signal since the magnetic enhancement of the palladium matrix is destroyed by the hydrogenation process. Unfortunately the self-heating of the lattice and its low thermal conduc-

TABLE II. Free paramagnetic NO function  $H_2^{5/2}$  for different applied fields and temperatures.

$1/T$ ( $\text{K}^{-1}$ )	$H$ (Oe)		
	50	200	500
333	88.5	203	283
200	92.6	210	286
143	93.5	216	289
100	91.2	222	293
66	83	223	298

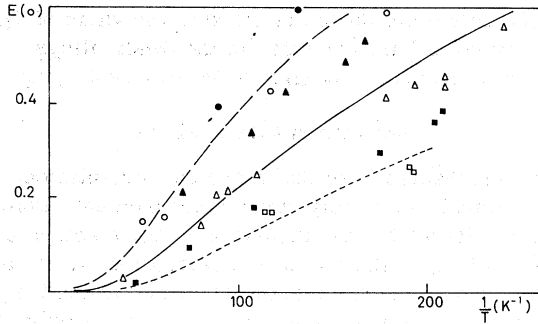


FIG. 2. 835-keV  $\gamma$ -ray axial anisotropy of  $^{54}\text{Mn}$  dissolved in palladium and gold as a function of  $1/T$  for  $H=50, 100, 200$  Oe. The curves represent the corresponding free-spin value  $E_2^{5/2}$  without taking into account any magnetic enhancement. The symbols are defined in the following table.

$H$ (Oe)	$C$	AuMn < 10	PdMn 3	$E_2^{5/2}$
50		□	■	----
100		△	▲	-----
200		○	●	-----

$C$  is the iron concentration per ppm, the same symbol is used for Figs. 3-5.

tivity precluded any absolute measurements; the main result is the appearance of a Kondo coupling defined by  $T_K \sim 20$  mK. Similar effects were observed in PdHCo alloys, the Kondo coupling reaching a value 2K.) As has been observed, the  $^{54}\text{Mn}$  in gold results are close to  $E_2^{5/2}$ .<sup>6,7</sup> The response of  $^{54}\text{Mn}$  in palladium is strongly enhanced from the free-spin function ( $S = \frac{5}{2}, g = 2$ ), which will characterize the local moment of manganese without an enhancement of the local electronic Zeeman term ( $gS > 5$ ).

Figure 3 shows that, down to 10 mK, the PdMn experimental results follow the enhanced function  $H_g^S$  with  $S = \frac{5}{2}, g = 3$ . This fit corresponds to a 7.5  $\mu_B$  giant moment in agreement with higher-temperature susceptibility results<sup>2</sup>; no concentration effects are detected in the value of the giant moment. It must be emphasized here that  $g$  is only a phenomenological parameter, which represents the positive shift ( $\alpha g_0$ ) of the local impurity value ( $g = g_0$ ) due to ferromagnetic exchange coupling between the highly correlated  $d$  conduction band and the local moment:

$$g = g_0(1 + \alpha).$$

Finally we mention that incorrect dynamical arguments, based on the comparison between the nuclear period  $\tau_n$  and the electronic relaxation time  $\tau_s$ , were previously invoked to describe the decoupling of  $I$  and  $S$  in NO. They are conceptually

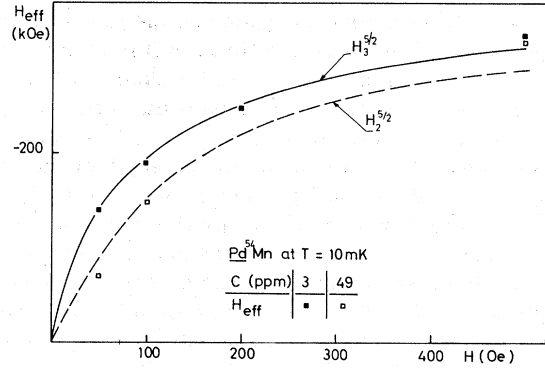


FIG. 3. At 10 mK, for two different concentrations of parasitic iron atoms, the variation of the effective field  $H_{\text{eff}}$  of  $^{54}\text{Mn}$  in PdMn alloys as a function of the applied field  $H$  is compared with the enhancement function  $H_3^{5/2}$ .

wrong as a NO experiment is a static experiment. An excellent experimental verification is provided by the present results since, although  $\tau_s \sim 10^{-9}$  sec (Ref. 10) is faster than  $\tau_n \sim 2 \times 10^{-8}$  sec,  $H_{\text{eff}}$  does not follow the Brillouin behavior given by the hypothesis of a dynamical decoupling. The fact that the NO results can be fitted to a  $H_g^S$  function is characteristic of a weak Kondo coupling ( $k_B T_K \ll A$ ); the local moment is strongly coupled to the nuclear spin and an eventual Kondo Hamiltonian is only a perturbing term for the electron nuclear sublevels.<sup>2</sup>

#### INTERACTION EFFECTS

The magnetic coupling among the iron impurities may affect the Mn behavior. For a sample of PdMn containing a higher concentration of iron (49 ppm), at 10 mK  $H_{\text{eff}}$  is strongly reduced in low fields from the  $H_3^{5/2}$  function. This attenuation is due to spin-glass interactions among the magnetic iron and manganese impurities as is suggested by Fig. 4 which shows the decrease of  $H_{\text{eff}}$  vs  $1/T$ . As for  $H > 500$  Oe the two samples give the same ef-

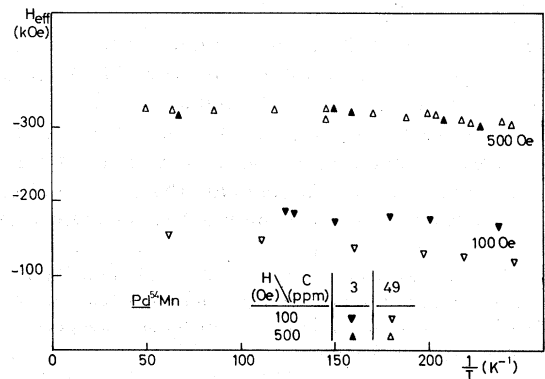


FIG. 4. Variation of the effective hyperfine field of  $^{54}\text{Mn}$  as a function of  $1/T$  for  $H=100, 500$  Oe.

fective field, we can conclude that, for  $H > 500$  Oe, all the iron impurities are completely saturated with a molecular field lower than 500 Oe. These results are confirmed by our magnetization measurements which show a full saturation for  $H = 600$  Oe at 55 mK. At low content of impurities, the magnetic interactions are not restricted to the ferromagnetic range of the electronic polarization, spin-glass behavior occurs. These results agree with Chouteau's magnetization experiments on PdFe alloys,<sup>11</sup> which show at low concentration (i) a main ferromagnetic pair coupling (ii) the occurrence of a molecular field not restricted to the ferromagnetic coupling.

In an unenhanced lattice like gold, for the same content of magnetic 3d impurities, the saturation of the magnetization is achieved in higher fields than those observed here: for example in a AuMn alloy with a 49 ppm impurity concentration, the saturation is not achieved in a field of 10 kOe.<sup>12</sup> The easy saturation observed here for the palladium matrix may reflect a low electronic spin polarization outside the giant moment range.

The sensitivity of NO experiments to the magnetic interaction effects appears clearly in Fig. 5 where at 5 mK even for the more dilute sample,  $H_{\text{eff}}$  deviates from the  $H_3^{5/2}$  function although the amplitude of the molecular field is very weak since (i) the susceptibility of the same sample follows a pure Curie law without Curie-Weiss behavior down to 50 mK; (ii) its magnetization follows a  $B_2^5$  Brillouin function. As was emphasized previously, the main effect observed by NO is the breakdown of the symmetry defined in the paramagnetic regime by the applied field.

Finally, Fig. 2 shows that below 10 mK the anisotropy of the AuMn alloy also deviates from the free-spin function  $E_2^{5/2}(0)$  although the presence of parasitic iron impurities cannot be detected in a magnetization experiment ( $C_{\text{Fe}} < 10$  ppm) and the manganese content is lower than 1 ppm. A magnet-

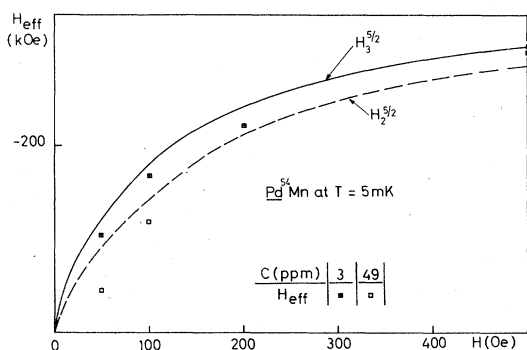


FIG. 5. Variation of the effective field  $H_{\text{eff}}$  of  $^{54}\text{Mn}$  in PdMn as a function of the applied field  $H$  at 5 mK.

ic Mn-Fe coupling seems to be ruled out as the iron impurity in gold is in a strong nonmagnetic singlet Kondo state ( $T_K \sim 400$  mK); the reduction of the anisotropy seems presumably due to the coupling among the Mn impurities. At the present time, we have no sure interpretation of the  $H_2^{5/2}$  deviation since we have found experimentally that the Au $^{54}\text{Mn}$  results are very sensitive below 10 mK to the sample preparation even for the same content of parasitic magnetic impurities: the main problem seems to be that of obtaining a homogeneous distribution of manganese impurities in the matrix (the practical consequence is that a Au $^{54}\text{Mn}$  NO thermometer must be always checked with a primary thermometer).

#### CONCLUSION

The giant moment of PdMn is characterized only by its enhanced polarization without any detectable Kondo-like coupling down to 10 mK. This is the first observation in NO of the enhanced electronic polarization which appears clearly as an enhancement of the electronic Zeeman term: the same effect has been observed previously in Mössbauer experiments performed on PdFe alloys<sup>13</sup> at higher temperatures.

This observation confirms experimentally that, in the weak Kondo coupling ( $A \gg k_B T_K$ ), the occurrence of a giant moment appears directly in NO experiment. It supports strongly the analysis made for the PdCo alloys<sup>14</sup> where the strong reduction of the NO signal from the enhanced function  $H_{10}^1$  corresponding to the  $10\mu_B$  giant moment was interpreted as the existence of a Kondo-like coupling.

As the susceptibility of the alloy containing less iron atoms follows a pure Curie law, the iron impurity like the manganese impurity is characterized by a very low Kondo temperature ( $T_K < 10$  mK) in contrast to the PdCo and PdNi alloy.<sup>11,14</sup>

Finally, because of the rather high values of  $I$  and  $S$  ( $I=3$ ,  $S \sim 2.5$ ) the free-spin function  $H_g^S$  is only sensitive to the product  $Sg$ . The choice of  $S=2.5$  and  $g=3$  is quite arbitrary for fitting the NO results. The fixed value  $S=\frac{5}{2}$  is in agreement with the linear response theory<sup>15</sup> and the recent ESR results of Alque *et al.*<sup>10</sup> who observe an unusual  $g$  shift ( $\Delta g \sim 0.6$ ) when the bottleneck with the conduction electrons is broken.

#### ACKNOWLEDGMENTS

The authors wish to thank Dr. I. A. Campbell, Dr. G. Chouteau, and Dr. R. Tournier for discussions and communication of results. One of us (J. S.) thanks the Centre de Recherche des Très Basses Températures laboratory for its hospitality during magnetization measurements. The authors are greatly indebted to J. Palaud for carrying out the neutron analysis.

- <sup>1</sup>W. M. Star, S. Foner, E. McNiff, Jr., Phys. Rev. B 12, 2690 (1975).
- <sup>2</sup>J. Flouquet, Ann. Phys. 8, 5 (1973-1974); and Prog. Low Temp. (to be published).
- <sup>3</sup>O. Taurian, thesis (Orsay, 1975) (unpublished).
- <sup>4</sup>A. Benoit and J. Sanchez (unpublished).
- <sup>5</sup>F. T. Avignone and G. D. Frey, Rev. Sci. Instrum. 39, 1941 (1968).
- <sup>6</sup>I. R. Williams, thesis (Oxford, 1968) (unpublished).
- <sup>7</sup>I. Legendijk, L. Niesen and W. J. Huiskampf, Phys. Lett. 30A, 326 (1969).
- <sup>8</sup>D. A. Shirley, Ann. Rev. Nucl. Sci. 16, 89 (1966).
- <sup>9</sup>J. Gallop, thesis (Oxford, 1970) (unpublished).
- <sup>10</sup>G. Alquie, A. Kreissler, and J. P. Burger, J. Less Common Met. 49, 97, 1976; and (unpublished).
- <sup>11</sup>G. Chouteau, thesis (Grenoble, 1973) (unpublished); G. Chouteau and R. Tournier, J. Phys. 32, 1002 (1971).
- <sup>12</sup>B. Manhes, thesis (Grenoble, 1971) (unpublished).
- <sup>13</sup>P. P. Craig, D. E. Nagle, W. E. Steyert, and R. D. Taylor, Phys. Rev. Lett. 9, 12 (1972).
- <sup>14</sup>J. Flouquet, O. Taurian, J. Sanchez, M. Chapellier, and J. L. Tholence, Phys. Rev. Lett. 38, 81 (1977).
- <sup>15</sup>S. Doniach and E. P. Wohlfarth, Proc. R. Soc. A 296, 442 (1967).